

PyRe: A Cyclus Pyroprocessing Facility Archetype

Gregory T. Westphal* and Kathryn D. Huff

Dept. of Nuclear, Plasma and Radiological Engineering, University of Illinois at Urbana-Champaign
*gtw2@illinois.edu

ABSTRACT

This work assesses system parameters that influence separation efficiency and throughput of pyroprocessing facilities. We leverage these parameters to implement a customizable pyroprocessing facility *archetype*, PyRe, for use with the Cyclus framework. This generic facility model will allow simulations to quantify signatures and observables associated with various operational modes and material throughputs for a variety of facility designs. Such quantification can aid timely detection of material diversion. This paper describes the facility archetype design, pyroprocessing flowsheets captured by the model, and simulation capabilities it enables. To analyze data retrieved from the model, we additionally propose a class for tracking and observing signatures and observables which will be extensible for other facility archetypes in the future.

INTRODUCTION

The diversion of significant quantities of SNM from the nuclear fuel cycle is major non-proliferation concern [1]. These diversions must be detected in a timely manner using signatures and observables in order to properly safeguard the fuel cycle. Timely detection is critical in non-proliferation to discover these shadow fuel cycles before diverted material is further processed. Pyroprocessing is a used nuclear fuel separations technology for advanced reactors. Signatures and observables are used to detect diversion of nuclear material. The goal of this research is to identify potential signs of material diversion in a pyroprocessing facility and implement models of these processes into a detailed pyroprocessing facility archetype to the modular, agent-based, fuel cycle simulator, CYCLUS [2]. This facility archetype will equip users of the CYCLUS fuel cycle simulator to investigate detection timeliness enabled by measuring signatures and observables in various fuel cycle scenarios.

BACKGROUND: CYCLUS

CYCLUS models the flow of material through user-defined nuclear fuel cycle scenarios. Facilities in nuclear fuel cycles vary, requiring a diverse collection of pre-designed facility process models, known as *archetypes*. CYCAMORE, the CYCLUS Additional MOdules REpository, provides common facility archetypes (separations, enrichment, reactor, etc.) [3]. Archetypes are customizable agent models which populate the simulation. Exact isotopes are dynamically tracked between facilities in discrete time steps [2]. This work seeks to add signature and observable tracking capabilities to CYCLUS. Potentially trackable signatures and observables include truck deliveries and power draw [4, 5]. This list is expanded upon in Table I to include pyroprocessing parameters.

PYROPROCESSING

Pyroprocessing is an electrochemical separation process used to recycle spent fuel into metallic fuel for use in advanced reactors. Separation efficiencies differ according to pyroprocessing facility design and fuel type. There are four major pyroprocessing systems with observable waste: voloxidation, electroreduction, electrorefining, and electrowinning [6].

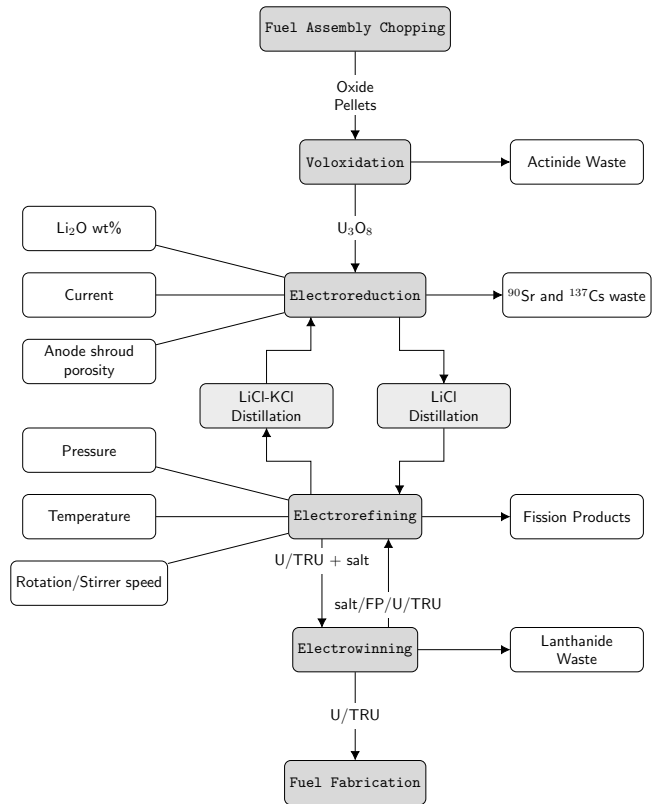


Fig. 1. An archetype design flowchart of pyroprocessing facilities including observable outputs and CYCLUS variables.

Figure 1 demonstrates the primary separations steps involved in a general pyroprocessing facility. Main process parameters are placed to the left of their respective subprocess. Boxes on the right side of the processes contain the observable waste produced by each step that PyRe tracks. The explicit behavior of each main process is described below.

Voloxidation

LWR fuel must be treated and separated before proceeding with electrolytic processes. Uranium dioxide heated to 500°C is converted to U_3O_8 while noble gases, carbon, and

tritium are collected to decay in storage. Actinides are also converted to their stable oxide forms and a majority are removed [7, 8]. Heating uranium dioxide above 800°C increases voloxidation throughput. Cycling oxidants between H₂ and air also improves the U₃O₈ reaction rate [8].

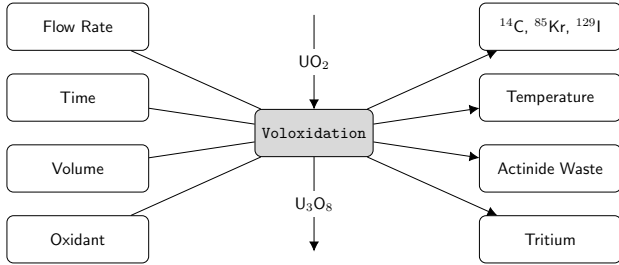


Fig. 2. A material balance over the voloxidation sub-process, including observables.

Electroreduction

The oxidant is converted into metallic fuel through electroreduction to be further refined through electrorefining and electrowinning. Yellowcake, created in voloxidation, enters the cathode, a negatively charged metal basket. A current density between 100 and 500 mA/cm² is applied to the anode in a molten LiCl salt. The electrolytic reduction process primarily results in diffusion of Cs, Ba and Sr, along with reduction and conversion of zirconium into metallic form [9, 7]. Electroreduction can further improve its throughput by adding Li₂O as a catalyst; this catalyst also prevents dissolution of the anode [9]. Since Li₂O is used to speed up the reaction, the operators could add more oxide than reported to International Atomic Energy Agency (IAEA). More frequent shipments of lithium oxide can be tracked as an observable to match records.

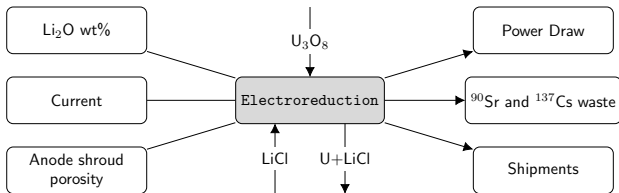


Fig. 3. A material balance over the electroreduction process with signatures and observables.

The Cesium and Strontium stream has a considerable decay signature proportional to the efficiency and size of the feed batch [6, 7].

Electrorefining

Once in metallic form, electrorefining electrochemically separates uranium and for fuel fabrication. The uranium and salt mixture from reduction is fed into an anode basket suspended in a graphite cathode. A LiCl-KCl eutectic is used as an electrolyte above 500°C [7, 10]. Uranium dissolves at the anode to recombine at the cathode as metallic uranium.

Waste transuranics (TRUs) and lanthanides are in a soluble chloride form while fission products and cladding remain in the anode basket. Finally, actinides and fission products are removed from the cladding electrochemically [10].

Lee et al. [11] show decreasing system pressure improves removal efficiency. Temperature, however, exhibits the opposite effect: as temperature decreases so does salt removal. This comes into effect particularly depending on material choice of instrumentation and containment [11]. Iron, for example, limits operating temperature because a eutectic forms at 725°C [12]. In facilities where iron equipment is present, temperatures are limited to 700°C, hindering efficiency. Cathode arrangement and anode rotation speed also affect the collection of uranium dendrites [11]. A central stirrer mixes uranium dendrites stuck on the vessel, improving separation efficiency and increasing throughput.

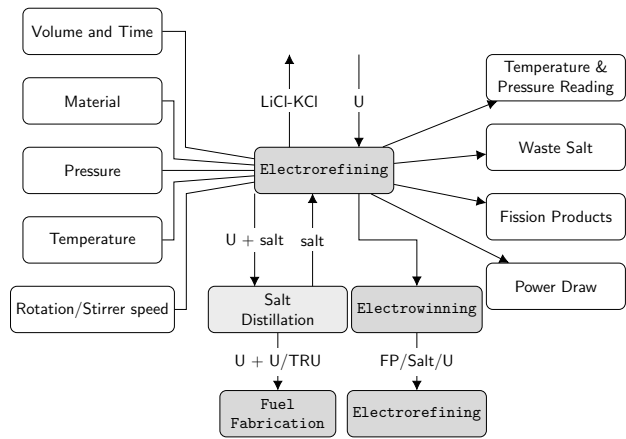


Fig. 4. A material balance over the electrorefining sub-process, including observables.

The electrorefining process also produces a fission product waste stream which requires monitoring. The following products are produced and tracked in PyRe at this step: Tc, Ag, Pd, Rh, Ru, Mo and Zr [7]. Uranium and TRU product streams separated at this stage are sent to fuel fabrication, while the remaining salt is reformed as an oxidant and recirculated. Separation efficiencies are taken after recirculation, and treated as a once-through cycle. Cyclus' time step is not detailed enough to benefit from analyzing intra-batch processes. Therefore, only end-state efficiencies are used rather than an explicit model.

Electrowinning

Molten salt containing TRUs from electrorefining is separated through electrowinning. This process separates trace uranium quantities, lanthanides and fission products. At 500°C there is approximately 99 wt% reduction in actinides and lanthanides [7]. Throughput also depends on material choice for the inert electrodes, impacting separation efficiency [13]. A shroud surrounds the anode to provide a path for O²⁻ ions to the anode and prevent Cl₂ from corroding the anode [14, 9]. Optimum operating current depends on material choice for the

anode shroud since a nonporous shroud limits ion pathways to the anode contact points. Higher porosity corresponds to free ion paths and a higher current. Increased currents reduce the separation time for electroreduction and electrowinning [9].

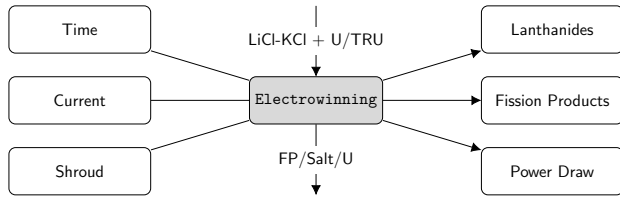


Fig. 5. A material balance over the electrowinning sub-process, including observables.

Figure 5 shows that electrowinning product recirculates to electrorefining after removing lanthanides. Fission products remaining in the salt from electrorefining are also removed here. In addition to physically tracked quantities, facility power can also be monitored to observe the use of current to increase throughput.

METHOD: CYCLUS SIMULATION

The separations facility provided by the CYCAMORE library is used as an initial model of a simple Pyroprocessing Integrated Demonstration (PRIDE) facility. Users provide the separations archetype with a feed stream and facility efficiencies. Each waste stream requires a material balance over voloxidation, electroreduction, electrorefining and electrowinning. Main waste streams are metallic waste, ceramic waste from electrowinning and electroreduction, and vitrified waste. Vitrified waste contains the majority of s, Sr, and rare-earth elements. Elemental separation efficiencies are determined through theoretical material balance determined by the NEA and Hermann et al [7, 15]. The simple simulation using a separations facility was run to verify the table of efficiencies input to CYCLUS. A scenario was created of one separations facility with a feed of five year cooled spent LWR fuel at a burn-up of 45 Gigawatt Days (GWd) per metric ton of initial heavy metal (MTIHM) to match results seen in [7].

A pyroprocessing facility can be modeled with the separations archetype at low fidelity. The goal for PyRe is to include facility configuration parameters and provide the user with data to optimize detector placement. PyRe accomplishes this by performing detailed separations at each subprocess and compiling the resulting streams. Any material not separated by the four processes is categorized as leftover commodity, ensuring material conservation is maintained. Unit tests and runtime checks will confirm material conservation.

Parameters

Facility configuration parameters customize the pyroprocessing archetype and vary by design. These pyroprocessing designs vary in multiple aspects which affect the throughputs and efficiencies of different waste streams. Table I compiles efficiency parameters for each sub-process.

Signatures and observables contain quantities measured

TABLE I: Archetype inputs and signatures & observables at each sub-process.

Sub-process	Parameters	S & O	Refs
Voloxidation	Volume	Tritium	[8]
	Oxidant	^{14}C	[7]
	Flow Rate	^{129}I	
	Temperature	^{85}Kr	
	Time	Actinides	
Electroreduction	Volume	^{90}Sr	[6]
	Batch Size	^{135}Cs	[7]
	Li_2O wt%	^{137}Cs	[9]
	Current	Power	[10]
		Draw	
	Porosity	Shipments	[16]
Electrorefining	Distillation Speed	Throughput	
	Time		
	Volume	Fission	[11]
		Products	
	Time	Power	[10]
Electrowinning		Draw	
	Material	Waste Salt	[7]
	Anode Rotation	Vacuum	[13]
		Pressure	
	Stirrer Speed	Temperature	[14]
	Pressure	Throughput	
Electrowinning	Temperature		
	Current	Power	[7]
		Draw	
	Shroud Material	Cadmium	[10]
Electrowinning		Waste	
	Time	Fission	[6]
		Products	
Facility	Flow Rate	Lanthanides	
		^{135}Cs	
		^{137}Cs	
Facility	Throughput	Shipments	
	Batch Size	Parking Lot	
		Thermal Image	

directly inside the facility and indirect characteristics observables at distance. A broader category for the facility as a whole is also described for global parameters such as throughput and batch size. Since throughput is a facility observable, it is seen in a majority of the sub-processes. Reduction is limited by batch size therefore reducing the throughput of preceding steps to the electrochemical process. The finished product and cars in the parking lot also serve as an indicator to excess work being done. Thermal imaging, further, can determine the operational status of the facility.

DISCUSSION

Using a material balance area over electrorefining and electroreduction yields the majority of detectable waste from the electrochemical processes. Material balances over the

remaining processes are used to verify diversion did not occur. Fuel fabrication is also at high risk of diversion. Finished product can be diverted with no additional processing steps so a material balance area is also taken here.

Multiple scenarios must be considered to determine the most sensitive points for diversion. Each facility parameter must be varied to observe their effects, as well as using a limited number of material balance areas. Scenarios will be run that include various monitoring points with the goal of determining if excess material was produced and diverted.

For example, an increase in Cs production points to electroreduction and electrowinning. If both increase similarly then current is likely affected as these processes share an increase in efficiency with increased current. Further in this scenario, if Cs production increases while Sr does not, electrowinning must be the point at which parameters are altered. A set of these scenarios will be used for sensitivity and importance analysis on the generic pyroprocessing facility.

CONCLUSIONS

This analysis demonstrates the variability in pyroprocessing facilities and their affects on potential signatures and observables that will be tracked through a detailed archetype. CYCLUS also is outlined as a tool in detecting shadow fuel cycles through its agent-based simulation and modular facilities, allowing for variations in plant design. Modeling and simulation of shadow fuel cycles will be performed in the CYCLUS environment after creation of a library specific to the unique needs of electrochemical refinement. Data from these simulations with additional signatures and observables will inform detector placements and measurement points leading to more reliable diversion detection.

ACKNOWLEDGMENTS

This material is based upon work supported by the Department of Energy National Nuclear Security Administration under Award Number(s) DE-NA0002576 via the Consortium for Nonproliferation Enabling Capabilities.

Prof. Huff is supported by the Nuclear Regulatory Commission Faculty Development Program, the Blue Waters sustained-petascale computing project supported by the National Science Foundation (awards OCI-0725070 and ACI-1238993) and the state of Illinois, the NNSA Office of Defense Nuclear Nonproliferation R&D through the Consortium for Verification Technologies and the Consortium for Nonproliferation Enabling Capabilities (awards DE-NA0002576 and DE-NA0002534), and the International Institute for Carbon Neutral Energy Research (WPI-I2CNER), sponsored by the Japanese Ministry of Education, Culture, Sports, Science and Technology.

REFERENCES

1. Y. AMANO, "IAEA Safeguards: Serving Nuclear Non-Proliferation," (Dec. 2017).
2. K. D. HUFF, M. J. GIDDEN, R. W. CARLSEN, R. R. FLANAGAN, M. B. MCGARRY, A. C. OPOTOWSKY,

- E. A. SCHNEIDER, A. M. SCOPATZ, and P. P. H. WILSON, "Fundamental concepts in the Cyclus nuclear fuel cycle simulation framework," *Advances in Engineering Software*, **94**, 46–59 (Apr. 2016).
3. R. W. CARLSEN, M. GIDDEN, K. D. HUFF, A. C. OPOTOWSKY, O. RAKHIMOV, A. M. SCOPATZ, and P. WILSON, "Cycamore v1.0.0," (Jun. 2014).
4. E. HOU, Y. YILMAZ, and A. O. HERO, "Diversion Detection in Partially Observed Nuclear Fuel Cycle Networks," (2016).
5. Y. YILMAZ, E. HOU, and A. O. HERO, "Online Diversion Detection in Nuclear Fuel Cycles via Multimodal Observations," (2016).
6. R. A. BORRELLI, J. AHN, and Y. HWANG, "Approaches to a Practical Systems Assessment for Safeguardability of Advanced Nuclear Fuel Cycles," *Nuclear Technology*, **197**, 248–264 (Mar. 2017).
7. ORGANISATION FOR ECONOMIC CO-OPERATION AND DEVELOPMENT, "Spent Nuclear Fuel Reprocessing Flowsheet," *Nuclear Energy Agency* (Jun. 2012).
8. R. JUBIN, "Spent Fuel Reprocessing," Tech. rep., Oak Ridge National Lab. (ORNL), Oak Ridge, TN (United States) (2009).
9. E.-Y. CHOI and S. M. JEONG, "Electrochemical processing of spent nuclear fuels: An overview of oxide reduction in pyroprocessing technology," *Progress in Natural Science: Materials International*, **25**, 6, 572–582 (Dec. 2015).
10. H. LEE, J.-M. HUR, J.-G. KIM, D.-H. AHN, Y.-Z. CHO, and S.-W. PAEK, "Korean Pyrochemical Process R&D activities," *Energy Procedia*, **7**, 391–395 (2011).
11. H. LEE, J. H. LEE, S. B. PARK, Y. S. LEE, E. H. KIM, and S. W. PARK, "Advanced Electrorefining Process at KAERI," *ATALANTE* (May 2008).
12. L. CHAPMAN and C. HOLCOMBE, "Revision of the uranium-iron phase diagram," *Journal of Nuclear Materials*, **126**, 3, 323–326 (Nov. 1984).
13. T. KOYAMA, Y. SAKAMURA, M. IIZUKA, T. KATO, T. MURAKAMI, and J.-P. GLATZ, "Development of Pyro-processing Fuel Cycle Technology for Closing Actinide Cycle," *Procedia Chemistry*, **7**, 772–778 (2012).
14. T.-J. KIM, G.-Y. KIM, D. YOON, D.-H. AHN, and S. PAEK, "Development of an anode structure consisting of graphite tubes and a SiC shroud for the electrowinning process in molten salt," *Journal of Radioanalytical and Nuclear Chemistry*, **295**, 3, 1855–1859 (Mar. 2013).
15. S. D. HERRMANN and S. X. LI, "Separation and Recovery of Uranium Metal from Spent Light Water Reactor Fuel Via Electrolytic Reduction and Electrorefining," *Nuclear Technology*, **171**, 3, 247–265 (Sep. 2010).
16. H. J. LEE, H. S. IM, and G. I. PARK, "Modeling of oxide reduction in repeated-batch pyroprocessing," *Annals of Nuclear Energy*, **88**, 1–11 (Feb. 2016).